Rapid flipping between electrolyte and metallic states in ammonia solutions of alkali metals

Marco Vitek,[1] Igor Rončević,[1, 2] Ondrej Marsalek*,[3, a)] H. Christian Schewe*,[1, 4, b)] and Pavel Jungwirth*[1, c)]

[1)] *Institute of Organic Chemistry and Biochemistry of the Czech Academy of Sciences, Flemingovo nám. 2, 166 10 Prague 6, Czech Republic*

[2)] *Department of Chemistry, University of Oxford, Chemistry Research Laboratory, Mansfield Road, Oxford OX1 3TA, UK*

[3)] *Charles University, Faculty of Mathematics and Physics, Ke Karlovu 3, 121 16 Prague 2, Czech Republic*

[4)] *J. Heyrovský Institute of Physical Chemistry, Czech Academy of Sciences, Dolejškova 3, 18223 Prague, Czech Republic*

(Dated: 6 June 2024)

Insulator-to-metal transitions are among the most fascinating phenomena in material science, associated with strong correlations, large fluctuations, and related features relevant to applications in electronics, spintronics, and optics. Dissolving alkali metals in liquid ammonia results in the formation of solvated electrons, which are localised in dilute solutions but exhibit metallic behaviour at higher concentrations, forming a disordered liquid metal. The electrolyte-to-metal transition in these systems appears to be gradual, but its microscopic origins remain poorly understood. Here, we provide a molecular-level time-resolved picture of the electrolyte-to-metal transition in solutions of lithium in liquid ammonia, employing ab initio molecular dynamics and many-body perturbation theory, which are validated against photoelectron spectroscopy experiments. We find a rapid flipping with a ∼40 fs timescale between metallic and electrolyte states within a broad range of concentrations. These flips are characterised by abrupt opening and closing of the band gap, which is connected with minute changes in the solution structure and the associated electron density distribution.

1. INTRODUCTION

The spectacularly colourful solutions of alkali metals in liquid ammonia have attracted attention of researchers since the 19th century (for a comprehensive review see Ref. [1], [2]). At lower alkali metal concentrations, the resulting deep blue solutions contain localised solvated electrons and dielectrons,[1,3–5] which found practical application as reducing agents for the hydrogenation of aromatic hydrocarbons within the Birch reduction process.[6] At higher concentrations, as the excess electrons become delocalised, the solution turns into a liquid metal with a characteristic golden metallic sheen and conductivity comparable to that of copper.[1,4,5]

Models of the nonmetal-to-metal transition in liquid systems go back to the work of Landau and Zeldovich in the 1940s[7] and have been experimentally tested on supercritical mercury or alkali metals numerous times.[8] The emerging picture has been that of a sharp transition occurring around the critical point, at which metal clusters of sufficient size are formed in the dense supercritical vapour. However, the behaviour of alkali metals dissolved in liquid ammonia is qualitatively different. In these systems, the nonmetal-to-metal transition happens gradually, merely with an increase of the concentration of electrons dissolved in a dense liquid.

Thus, we refer to this liquid state phenomenon as the electrolyte-to-metal transition (EMT). In contrast to supercritical mercury,[8] alkali metals dissolved in liquid ammonia do not exhibit a sharp transition, but a gradual one in the concentration range of about 1–10 MPM (mole percent metal; in liquid ammonia, 1 MPM equals to roughly 0.4 M).[2,5]

Three historical models have been suggested for the EMT in alkali metal-liquid ammonia systems:[2] (i) a percolation model based on experimental findings of microscopic inhomogeneities,[9] (ii) an extension of the Landau and Zeldovich model introducing a critical electron density for metallisation,[10,11] and (iii) a model linking the transition to a polarisation catastrophe.[12] Despite these efforts, the molecular mechanism underlying the EMT remains inconclusive.

A phenomenon that has been closely connected to the EMT mechanism concerns inhomogeneities or fluctuations of concentration occurring in the alkali metal-ammonia solutions in the intermediate range of 1–8 MPM.[13,14] Experimental evidence for microscopic structural inhomogeneities was first provided by X-ray diffraction studies.[15] Subsequently, large concentration fluctuations in lithium and sodium ammonia solutions were deduced from investigations of the dependence of the chemical potential on the alkali metal concentration.[16] Finally, the nanometer-sized correlation lengths of the fluctuations were derived from small-angle neutron scattering studies.[17] Based on these experimental studies, a model was proposed suggesting the coexistence of dilute and concentrated voids in the intermediate concentration regime, which accounted for the spatial dimensions of the inhomogeneities.[18] However, no temporal information about these fluctuations has been provided so far,

———————

a)Electronic mail: ondrej.marsalek@mff.cuni.cz
b)Electronic mail: hanns_christian.schewe@uochb.cas.cz
c)Electronic mail: pavel.jungwirth@uochb.cas.cz

neither experimentally nor from modelling,[2,19] making it hardly possible to deduce their molecular origins.

In such a situation, molecular dynamics (MD) simulations can serve as a very useful tool with an arbitrary spatial and temporal resolution, provided the underlying interactions are described with sufficient rigour and accuracy. For the present systems containing solvated electrons, a quantum description of the electronic structure is imperative. The first application of molecular dynamics to the EMT in alkali metal-liquid ammonia systems accomplished 30 years ago had to resort — due to limited methodology and computational resources available at the time — to semi-empirical methods for the description of the interactions of the excess electrons among themselves and with the rest of the system.[20] This severe approximation strongly limited both the range of accessible electronic structure scenarios and the fidelity of the predictions. In this study, we overcome the above limitations by employing *ab initio* molecular dynamics (AIMD) with an explicit quantum mechanical description of all the excess and valence electrons in the system based on the density functional theory (DFT) and the one-body Green's function (GW) approximation. The use of a state-of-the-art hybrid density functional for MD ensures that our trajectories are faithful, while the GW method provides accurate electronic structure information via a post-DFT description of Coulombic screening. This simulation methodology is suficiently robust to describe the dynamics and electronic structure of highly concentrated metallic solutions.

The present simulations, validated against existing experimental data, allow us not only to follow the ongoing molecular dynamics of all the species present in the solution but also to track the changes in the electronic structure of the investigated systems on a femtosecond scale. In this way, we are able to fill the existing knowledge gap concerning the temporal molecular-scale behaviour of solutions of alkali metals in liquid ammonia.

As a key result for the understanding of the dynamics of the EMT, we observe and quantify fast flipping between metallic and non-metallic states on an average time-scale of about 40 fs.

2. RESULTS & DISCUSSION

A. Density of states and spherical band structure

We designed the simulation framework in a way that allowed us to capture the two principal – and at the same time opposing – aspects of EMT. On the one hand, we aimed for the size of the unit cell to be large enough to cover the concentration regime ($\approx$ 1 - 10 MPM) where EMT takes place. On the other hand, since the average radius of the metallic and non-metallic domains pertinent to EMT has been estimated to be 15-25 Å,[9] the simulated unit cell should also be roughly commensurate with this size, i.e., small enough not to average out these structural inhomogeneities. Hence, we deliberately chose the size of the unit cell of about 15 Å containing at the experimental density 64 ammonia molecules with a varying number of solvated dielectrons and Li$^+$ cations to mimic concentrations of 3.0 - 11.1 MPM (for details see SI).

Figure 1 a-c shows representative snapshots taken from AIMD simulations at 3.0, 6.0 and 11.1 MPM, covering the EMT concentration range. Complete trajectories obtained from AIMD were then used to calculate the averaged densities of states (DoS) using the G_0W_0 method[21,22] (for details see SI) as presented in Figure 1 e,g,i. We see a progressive narrowing and filling of the gap between the highest occupied and lowest unoccupied orbitals as the concentration of the alkali metal increases with rising density at the Fermi level as a signature of the gradual EMT.

Next, we quantify the relationship between the energy of electrons and their momentum which is typically represented by the band structure of a material. However, in (disordered) liquid metals the first Brillouin zone cannot be rigorously defined,[23–26] in contrast to periodic structures of crystalline solids. Nevertheless, a radial band structure has previously been measured, e.g., in a lead monolayer melted on a silicon surface.[27] Analogously, we introduce here the concept of a radial band structure in 3D. Denoted here as a spherical band structure (SBS), it represents the energy-momentum relationship in a spherically symmetrical space, where the electron energy is plotted versus the magnitude of the wave vector k.

The SBSs presented in Figure 1 d,f,h were obtained from 100 AIMD snapshots for each concentration (for further details see SI). They provide a more detailed picture than the DoS of the structure of the band gap and its gradual narrowing and filling with increasing alkali metal concentration. SBS also lends further insights into EMT, providing information about the electron energy and momentum dispersion relations. In the following, we first perform a detailed temporal analysis of the AIMD data. Finally, we compare the calculated DoS with our reanalysed experimental data.

B. Rapid flipping dynamics

While Figure 1 depicts SBSs and DoSs averaged over 100 geometries, analysing the results for individual snapshots allows us to distinguish between electrolyte and metallic configurations along the AIMD trajectory. This analysis reveals that metallic states appear in about 40 % of all snapshots already at 3.0 MPM, with a similar fraction of metallic frames appearing also at 6.0 MPM (see SI for a further quantitative analysis of the observed bimodal distribution distinctly categorising the snapshots as metallic or non-metallic). At 8.5 MPM and above, all the configurations are metallic, evidencing a completed transition to the metallic state, in agreement with previous experimental results.[5]

Let us now return to the intermediate concentration
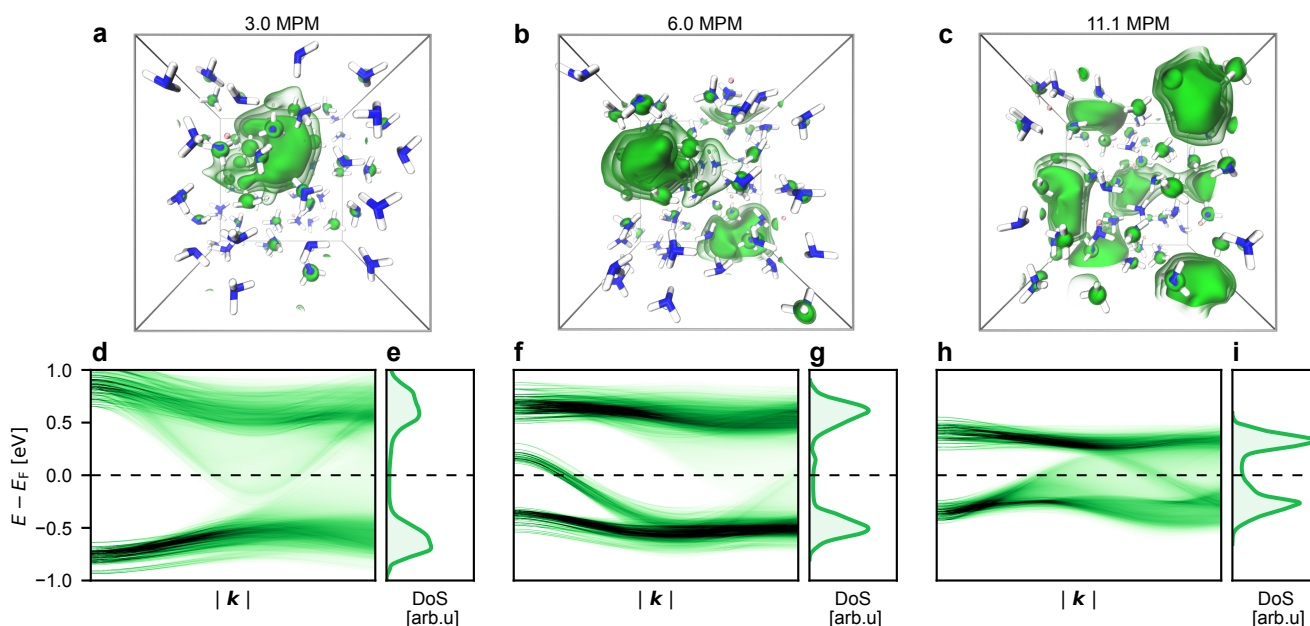
Figure 1. Representative AIMD simulation snapshots and corresponding electronic properties of alkali metal-ammonia solutions at various concentrations. The top panels show the simulation box for concentrations of a) 3.0 MPM, b) 6.0 MPM, and c) 11.1 MPM, illustrating the spatial distribution of solvated electrons within the solvent. The bottom panels display the corresponding SBS (d,f,h) and associated DoS (e,g,i). For clarity, only the valence and conduction bands near the Fermi level (black dashed line), E_F, are displayed.
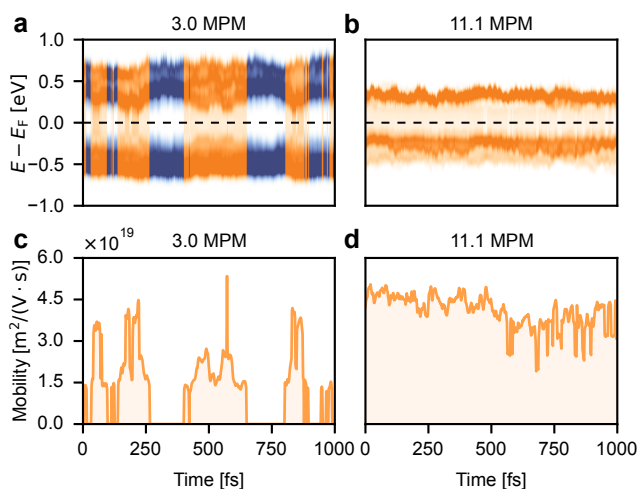
Figure 2. Temporal evolution of (a,b) the DoS and (c,d) electron mobility in AIMD snapshots at a 3.0 and 11.1 MPM, sampled every 2 fs.

regime of 3.0 MPM, where the system flips fast between electrolyte and metallic states. From the EMT perspective, this regime is not only interesting for simulations but also from the point of view of experimental measurables such as the electrical conductivity or the related electron mobility, which are found to be highly dependent on concentration.[2,28] To probe these transport properties, we analysed 500 configurations sampled from AIMD trajec-

tories in 2 fs intervals at 3.0 MPM (intermediate regime) and 11.1 MPM (metallic regime). For both concentrations, Figure 2 shows the corresponding time evolutions of the simulated DoS and electron mobility (see Methods for details). Our main finding is that the average time interval between flips from an electrolyte to a metal and vice versa is only a few tens of femtoseconds, namely 39 fs at 3.0 MPM. Moreover, the flipping seems to be happening in a quasi-random fashion, i.e., without a characteristic frequency, which exhibits a relatively broad distribution of time intervals the system spends in either of the two states. In contrast, at 11.1 MPM all configurations manifest a metallic behaviour with no transition to the electrolyte states.

Next, we made an attempt to identify potential structural differences that may relate to the observed bimodal distribution of metallic and electrolyte states at 3.0 MPM. To this end, we examined 1000 configurations sampled every 20 fs from 4 AIMD trajectories at this concentration, to determine which snapshot corresponds to an electrolyte or a metal. Figure 3 a,b demonstrates that the excess electron densities for subsequent electrolyte and metallic configurations overlap strongly. Nevertheless, for separately averaged electrolyte vs metallic configurations we see small but non-negligible alterations in the excess electron gyration radii and radial profiles, with the excess electron being slightly more spatially extended for the metal than the electrolyte (Figure 3 c,d).

To investigate the temporal dynamics of EMT in greater detail, we analyse the SBSs of two consecutive
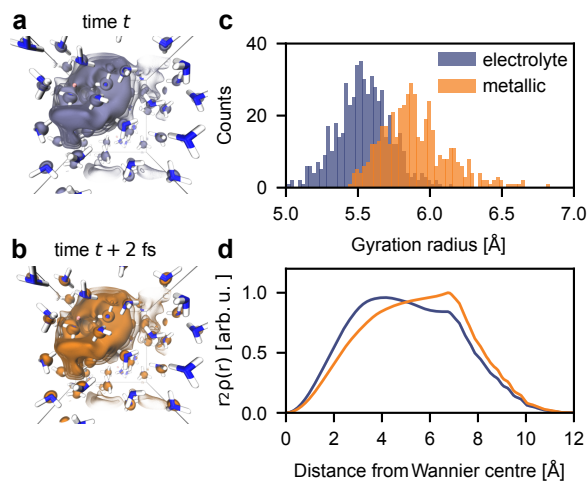
Figure 3. Analysis of solvated dielectron density and volumetric properties in 3.0 MPM alkali metal-ammonia solution. Panels (a) and (b) depict the electron density configurations of the dielectron in the electrolyte and metallic states, respectively, with snapshots taken 2 fs apart. Panel (c) displays the radii of gyration, and Panel (d) illustrates the spherically integrated electron density profiles.
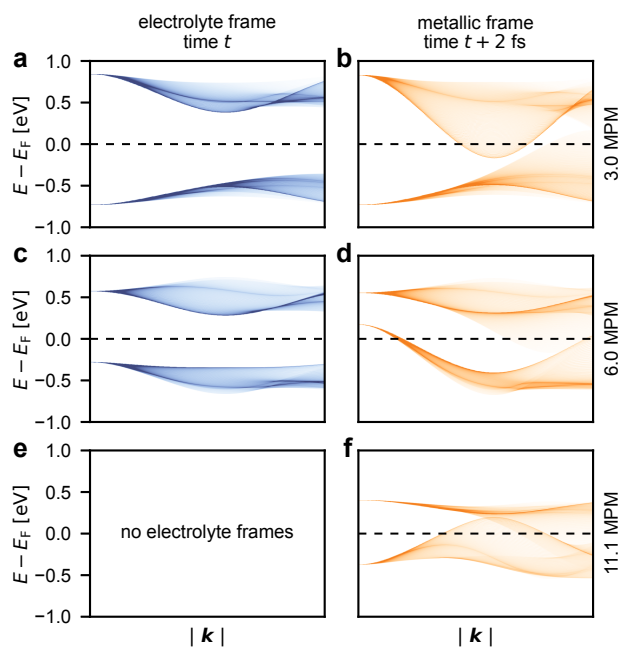
Figure 4. SBS of consecutive electrolyte (a,c,e) and metallic (b,d,e) frames at 3.0, 6.0, and 11.1 MPM. For clarity, only the valence and conduction bands near the Fermi level (black dashed line), E_F, are displayed.

snapshots separated by 2 fs on either side of the transition (Figure 4). At both 3.0 and 6.0 MPM we see large changes in the bands close to the Fermi level occurring during the flipping despite the fact that the atomic positions and electron densities right before and after the flip remain very close to each other. This indicates that the flipping is induced by only small changes in molecular geometries leading, nevertheless, to significant temporal fluctuations in the band gap, which appears to be just enough to switch between metallic and electrolyte behaviour. In other words, the width and degree of filling of the band gap in the present system turns out to be very sensitive to small changes in molecular geometry and the associated electron density distribution.

C. Experimental validation

In our recent study,[5] we combined the techniques of liquid micro-jets with synchrotron X-ray photoelectron (PE) spectroscopy to determine the binding energies and the densities of states of the excess electrons in liquid ammonia over a broad concentration range of 0.08-9.7 MPM. Figure 5 displays the DoS determined from the G_0W_0 calculations (refined using the Boltztrap2 code,[29,30] see SI) based on 100 AIMD snapshots at intervals of 200 femtoseconds from 4 trajectories for each of the two systems at 3.0 MPM and 11.1 MPM, plotted against experimental data[5] for direct comparison. The experimental PE spectra reveal a clear picture of a gradual EMT. Employing a fitting procedure has enabled quantification of the decrease of the solvated (di)electron peak pertinent to the electrolyte with a simultaneous rise of the metallic spectral features, i.e, the signatures of the conduction band as well as features corresponding to plasmonic oscillations, as the alkali metal concentration increases.[5]

The calculated DoSs align with experimental spectra at comparable concentrations of 3.4 and 9.7 MPM. Namely, at the higher concentration where the system is metallic all the time, both simulation and experiment exhibit an asymmetric peak corresponding to the conduction band sharply ending at the Fermi level (the slight offset of about 0.2 eV between the calculation and measurement is within the accuracy of the absolute calibration of the experiment). At the lower concentration, the calculated DoS can be separated into contributions from electrolyte and metallic snapshots. While this is not possible for the experiment which averages the signal over time, the measured PE signal can still be split (after subtracting features corresponding to plasmonic oscillations) into direct contributions from localised dielectrons and delocalised metallic electrons. We see that the signal calculated for the electrolyte snapshots aligns well with the experimental contribution from the dielectrons. The comparison for the metallic snapshots is less straightforward since the corresponding densities of states result from a superposition of localised and delocalised electrons. The latter contribution nevertheless aligns well with the measured "metallic part" of the spectrum. This general agreement between calculations and experiments underscores the suitability of G_0W_0 for capturing the essential physical phenomena associated with the EMT.
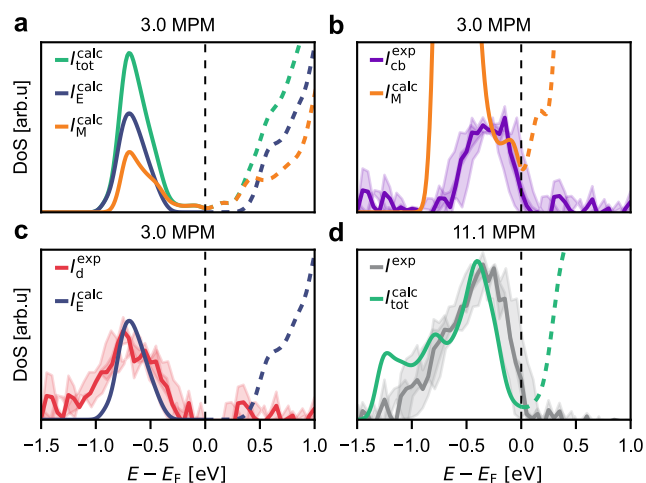
Figure 5. Comparative analysis of the calculated DoS with experimental PE spectroscopy data for an alkali metal-ammonia solution at two concentrations. (a) calculated DoS at 3.0 MPM, split into metallic (orange) and electrolyte (blue) contributions, alongside the total DoS (green). (b) comparison of the calculated metallic contribution (orange) with the experimental PE spectra of the isolated conduction band (purple). (c) calculated electrolyte contribution (blue) versus the experimental PE spectra of the dielectron only (red). Panel (d) compares the total DoS at an elevated concentration of 11.1 MPM (green) with experimental results at 9.7 MPM (grey).

3. CONCLUSION

We have characterised and quantified the ultrafast flipping dynamics between metallic and electrolyte states in concentrated solutions of lithium in liquid ammonia. This allows us to provide the key missing characteristics of these systems, namely, the mean time interval between these flips which turns out to be of the order of a few tens of femtoseconds. We show that band gap properties depend very sensitively on minor changes in molecular geometry and electron density, which then drive switching between a liquid metal and an electrolyte. Moreover, we demonstrate that the densities of states of metallic configurations still to a large extent possess features pertinent to electrolyte configurations, with only a weak filling of the band gap.

Ab initio molecular dynamics simulations proved to be a powerful tool for following the flipping between a liquid metal and electrolyte with atomistic resolution at a femtosecond timescale, the validity of which has been supported by an agreement between simulated and experimental photoelectron spectra of these systems. Direct measurements of the flipping phenomena may prove difficult due to the very small nanometer size of the metallic and electrolyte domains. Nevertheless, a feasible strategy to probe the flipping time indirectly may be a pump-probe experiment where one would follow the relaxation of the photoexcited system back to equilibrium. In order to attain the temporal as well as the spatial resolution

ultrafast (attosecond) X-ray diffraction[31] — a technology that is now becoming within reach — is likely to be a game changer.

4. METHODS

In this study, we utilised molecular dynamics simulations to investigate the electronic properties of ammonia solutions containing varying concentrations of solvated dielectrons and lithium cations. In order to generate initial configurations we employed force-field molecular dynamics (FFMD) simulations using a liquid-adapted ammonia force field.[32] These configurations then served as the starting point for production runs of AIMD utilising the VASP program package.[33–36] Within AIMD simulations, the electronic structure was described using the hybrid revPBE0-D3 functional.[37–40] For each system, multiple trajectories were generated, involving an equilibration phase followed by a production run to provide adequate sampling (for more details see SI).

To determine electronic structure variations along the trajectories, DoS calculations were performed using directly the revPBE0-D3 functional and using the G_0W_0 method. These calculations were performed employing either a single gamma point or a gamma-centred $2\times2\times2$ k-point mesh to provide an accurate representation of the electronic properties of the systems.

We employed BoltzTraP2[29,30] for evaluating electron mobilities based on the simulated electronic structures. Additionally, SBSs were generated for analysis of the electron energy dispersion in a spherically symmetric space. Taken together, the above computational approaches enabled a detailed time-resolved examination of the electronic structure of solvated electrons in liquid ammonia at a molecular level.

SUPPORTING INFORMATION

Supporting information contains supplementary computational methods, figures, and data.

ACKNOWLEDGEMENT

(ID:90254). We acknowledge ChatGPT for improving readability and language.

REFERENCES

[1] J. C. Thompson, *Electrons in liquid ammonia*, Monographs on the physics and chemistry of materials (Clarendon, 1976).

[2] E. Zurek, P. Edwards, and R. Hoffmann, "A molecular perspective on lithium–ammonia solutions," Angewandte Chemie International Edition **48**, 8198–8232 (2009).

[3] N. F. Mott, "Metal-insulator transitions in metal-ammonia solutions," The Journal of Physical Chemistry **84**, 1199–1203 (1980).

[4] S. Hayama, N. T. Skipper, J. C. Wasse, and H. Thompson, "X-ray diffraction studies of solutions of lithium in ammonia: The structure of the metal–nonmetal transition," The Journal of Chemical Physics **116**, 2991–2996 (2002).

[5] T. Buttersack, P. E. Mason, R. S. McMullen, H. C. Schewe, T. Martinek, K. Brezina, M. Crhan, A. Gomez, D. Hein, G. Wartner, R. Seidel, H. Ali, S. Thürmer, O. Marsalek, B. Winter, S. E. Bradforth, and P. Jungwirth, "Photoelectron spectra of alkali metal-ammonia microjets: From blue electrolyte to bronze metal," Science **368**, 1086–1091 (2020).

[6] A. J. Birch, "Reduction by dissolving metals," Nature **158**, 585–585 (1946).

[7] L. Landau and Y. B. Zeldovich, "On the relation between the liquid and the gaseous states of metals," Acta Physicochim. USSR **18**, 194–196 (1943).

[8] F. Hensel and E. U. Franck, "Metal-nonmetal transition in dense mercury vapor," Rev. Mod. Phys. **40**, 697–703 (1968).

[9] J. Jortner and M. H. Cohen, "Metal-nonmetal transition in metal-ammonia solutions," Phys. Rev. B **13**, 1548–1568 (1976).

[10] N. F. Mott, "The transition to the metallic state," The Philosophical Magazine: A Journal of Theoretical Experimental and Applied Physics **6**, 287–309 (1961).

[11] N. Mott, *Metal-Insulator Transitions* (Taylor & Francis, 1990).

[12] K. F. Herzfeld, "On atomic properties which make an element a metal," Phys. Rev. **29**, 701–705 (1927).

[13] J. C. Thompson, "Metal-nonmetal transition in metal-ammonia solutions," Rev. Mod. Phys. **40**, 704–710 (1968).

[14] M. H. Cohen and J. C. Thompson, "The electronic and ionic structures of metal-ammonia solutions," Advances in Physics **17**, 857–907 (1968).

[15] P. W. Schmidt, "Small Angle X-Ray Scattering from Solutions of Alkali Metals in Liquid Ammonia," The Journal of Chemical Physics **27**, 23–28 (2004).

[16] K. Ichikawa and J. C. Thompson, "Chemical potentials and related thermodynamics of sodium-ammonia solutions," The Journal of Chemical Physics **59**, 1680–1692 (2003).

[17] P. Chieux, "Small angle neutron scattering studies of concentration fluctuations in the non metal to metal transition range: solutions of 7li in nd3," Physics Letters A **48**, 493–494 (1974).

[18] M. H. Cohen and J. Jortner, "Metal-nonmetal transition in metal-ammonia solutions via the inhomogeneous transport regime," The Journal of Physical Chemistry **79**, 2900–2915 (1975).

[19] P. Damay and P. Schettler, "Fluctuations in metal-ammonia solutions," The Journal of Physical Chemistry **79**, 2930–2935 (1975).

[20] Z. Deng, G. J. Martyna, and M. L. Klein, "Quantum simulation studies of metal–ammonia solutions," The Journal of Chemical Physics **100**, 7590–7601 (1994).

[21] L. Hedin, "New method for calculating the one-particle green's function with application to the electron-gas problem," Phys. Rev. **139**, A796–A823 (1965).

[22] M. S. Hybertsen and S. G. Louie, "Electron correlation in semiconductors and insulators: Band gaps and quasiparticle energies," Phys. Rev. B **34**, 5390–5413 (1986).

[23] R. M. Stratt and B.-C. Xu, "Band structure in a liquid," Phys. Rev. Lett. **62**, 1675–1678 (1989).

[24] L.-W. Wang, L. Bellaiche, S.-H. Wei, and A. Zunger, ""majority representation" of alloy electronic states," Phys. Rev. Lett. **80**, 4725–4728 (1998).

[25] C. Zheng, S. Yu, and O. Rubel, "Structural dynamics in hybrid halide perovskites: Bulk rashba splitting, spin texture, and carrier localization," Phys. Rev. Mater. **2**, 114604 (2018).

[26] O. Rubel, A. Bokhanchuk, S. J. Ahmed, and E. Assmann, "Unfolding the band structure of disordered solids: From bound states to high-mobility kane fermions," Phys. Rev. B **90**, 115202 (2014).

[27] K. S. Kim and H. W. Yeom, "Radial band structure of electrons in liquid metals," Phys. Rev. Lett. **107**, 136402 (2011).

[28] M. Hirasawa, Y. Nakamura, and M. Shimoji, "Electrical conductivity and thermoelectric power of concentrated lithium-ammonia solutions," Berichte der Bunsengesellschaft für physikalische Chemie **82**, 815–818 (1978).

[29] G. K. Madsen, J. Carrete, and M. J. Verstraete, "Boltztrap2, a program for interpolating band structures and calculating semiclassical transport coefficients," Computer Physics Communications **231**, 140–145 (2018).

[30] F. Ricci, W. Chen, U. Aydemir, G. J. Snyder, G.-M. Rignanese, A. Jain, and G. Hautier, "An ab initio electronic transport database for inorganic materials," Scientific data **4**, 1–13 (2017).

[31] J. Kang, Y. Lee, S. Lee, H. Ki, J. Kim, J. Gu, Y. Cha, J. Heo, K. W. Lee, S. O. Kim, J. Park, S.-Y. Park, S. Kim, R. Ma, I. Eom, M. Kim, J. Kim, J. H. Lee, and H. Ihee, "Dynamic three-dimensional structures of a metal–organic framework captured with femtosecond serial crystallography," Nature Chemistry **16**, 693–699 (2024).

[32] D. Chakraborty and A. Chandra, "Voids and necks in liquid ammonia and their roles in diffusion of ions of varying size," Journal of Computational Chemistry **33**, 843–852 (2012).

[33] G. Kresse and J. Hafner, "Ab initio molecular dynamics for liquid metals," Phys. Rev. B **47**, 558–561 (1993).

[34] G. Kresse and J. Hafner, "Ab initio molecular-dynamics simulation of the liquid-metal–amorphous-semiconductor transition in germanium," Phys. Rev. B **49**, 14251–14269 (1994).

[35] G. Kresse and J. Furthmüller, "Efficiency of ab-initio total energy calculations for metals and semiconductors using a plane-wave basis set," Computational Materials Science **6**, 15–50 (1996).

[36] G. Kresse and J. Furthmüller, "Efficient iterative schemes for ab initio total-energy calculations using a plane-wave basis set," Phys. Rev. B **54**, 11169–11186 (1996).

[37] J. P. Perdew, K. Burke, and M. Ernzerhof, "Generalized gradient approximation made simple," Phys. Rev. Lett. **77**, 3865–3868 (1996).

[38] C. Adamo and V. Barone, "Toward reliable density functional methods without adjustable parameters: The PBE0 model," The Journal of Chemical Physics **110**, 6158–6170 (1999).

[39] Y. Zhang and W. Yang, "Comment on "generalized gradient approximation made simple"," Phys. Rev. Lett. **80**, 890–890 (1998).

[40] L. Goerigk and S. Grimme, "A thorough benchmark of density functional methods for general main group thermochemistry, kinetics, and noncovalent interactions," Phys. Chem. Chem. Phys. **13**, 6670–6688 (2011).